Research Article

Performance of the CUSUM Control Chart Using Approximation to ARL for Long-Memory Fractionally Integrated Autoregressive Process with Exogenous Variable

Direk Bualuang
Department of Mathematics, Faculty of Science and Technology, Uttaradit Rajabhat University, Uttaradit, Thailand

Wilasinee Peerajit*
Department of Applied Statistics, Faculty of Applied Science, King Mongkut's University of Technology North Bangkok, Bangkok, Thailand

* Corresponding author. E-mail: wilasinee.p@sci.kmutnb.ac.th DOI: 10.14416/j.asep.2022.05.003
Received: 5 January 2022; Revised: 21 February 2022; Accepted: 4 April 2022; Published online: 10 May 2022

Abstract
The cumulative sum (CUSUM) control chart is a well-known process monitoring tool that is sensitive to small-to-moderate changes in process parameters. In this paper, we propose an approximated average run length (ARL) method based on the numerical integral equation (NIE) method for monitoring the mean of a long-memory autoregressive fractionally integrated process with an exogenous variable (ARFIX) running on a CUSUM control chart. The approximated ARL based on the NIE method is realized by solving a system of linear equations and integration based on the partitioning and summation of the area under the curve of a function derived by using the Gauss-Legendre quadrature. In a comparative study with the ARL based on analytical formulas, the proposed approximated ARL method could detect shifts of various sizes in the process mean of an ARFIX process running on a CUSUM control chart. In addition, the proposed method was compared with their analytical formulas in terms of the relative percentage change (r%) to verify the accuracy of the ARL results. The results revealed that the ARL results obtained from the NIE method are an approach to analytical formulas with r% of less than 0.25. Hence, the NIE method is very accurate and in excellent agreement with the analytical formulas approach. Apparently, the NIE method is an alternative as efficiently as the analytical method for this situation. It also performed well in comparison with the approximated ARL for the same process running on an exponentially weighted moving average control chart. In addition, real datasets are also used to demonstrate the efficacy of the proposed method.

Keywords: Approximated ARL, Numerical integral equation, Gauss-legendre quadrature, CUSUM control chart, ARFIX

1 Introduction

Control charts are critical for monitoring processes in the production and manufacturing sectors. The Shewhart control chart is the most frequently used one due to its simplicity and excellent sensitivity to large changes in process parameters. On the other hand, it is poor at detecting small-to-moderate changes in process parameters, and as a result of this limitation, researchers have devised new control charts for this scenario, including two well-known ones being the cumulative sum (CUSUM) control chart [1] and the exponentially weighted moving average (EWMA) control chart [2].

Montgomery [3] demonstrated that the CUSUM control chart is a more efficient alternative to the Shewhart control chart for detecting small-to-moderate process parameter shifts. It is widely utilized in a wide range of fields and operations, including healthcare, manufacturing, credit card fraud detection, weather monitoring, and stock exchange trading.

The average run length (ARL) is the most widely used measure for evaluating control chart performance. To monitor a process efficiently, the in-control ARL (ARL_0) should be as large as possible, while no shift in the process parameter occurs and the out-of-control ARL (ARL_1) should be as small as possible when a shift in the process parameter occurs [4]. The current study aims to establish an approximation of the ARL by using the numerical integral equation (NIE) method for a process running on a CUSUM control chart.

Autocorrelation is a naturally occurring phenomenon that can have a significant effect on the performance of a control chart [5]–[7]. Nevertheless, it must be appropriately modeled and monitored. Jiang [8] analyzed the ARL of an autoregressive (AR) moving average (MA) (ARMA) control chart via an ARMA(1,1) model, while Lu and Reynolds [9] investigated the performance of a first-order AR (AR(1)) process running on a CUSUM control chart.

Several models of random processes with a time-series element have been developed. Autoregressive models have been applied in a wide variety of sectors. Yue and Pilon [10] examined annual mean daily streamflow data from 15 watersheds by using a linear trend in an AR(1) process. In Hamed's [11] study, hydrologic data was represented as an AR(1) process with a linear trend. In addition, Karaoglan and Bayhan [12] conducted a case study using a trend-stationary AR(1) model to determine the peroxide values of stored vegetable oil. Thus, a control chart can be used to examine the trend in an AR(1) model.

When constructing a model, it is extremely important to measure observational errors that defined as the difference between the actual and approximated values. Inferring a more efficient model requires small errors. White noise (or normally distributed white noise) is a broad term that refers to the errors in a time-series model with autocorrelated observations. An AR model with normally distributed white noise is a time-series model that is often used in many fields, such as economics [13]. However, white noise can be non-normally distributed, most commonly as exponential [14]–[18].

The above-mentioned models are for short-memory processes. For long-memory processes, we use the advanced concept of fractional integration when modeling, which has led to the development of multiple models, the most popular of which is the AR fractionally integrated MA(ARFIMA) model introduced by Granger and Joyeux [19]. ARFIMAX is an extension of ARFIMA with an exogenous variable [19], [20]. Ebens [21] proposed using an ARFIMAX model to predict changes in a Dow Jones Industrial Average portfolio and discovered correlations between econometric models and economic indicators (variables) that affect economic forecasting. Government investment policies, currency rates, interest rates, and inflation rates are all examples of exogenous variables that are independent of other variables in the system. These variables affect the econometric model's forecasting capability. If an exogenous variable is included in any sort of forecasting, the predictive power of the model will be greater than without it.

Numerous control charts have been used to construct models with a focus on the fractional integration process with time-series components. For example, Ramjee [22] used correlated data in Shewhart and EWMA control charts with an ARFIMA model. Although process shifts could be detected, the two control charts were found to be inefficient. Later, Ramjee *et al.* [23] introduced the forecast-based hyperbolic weighted MA(HWMA) control chart with a non-stationary ARFIMA model. Pan and Chen [24] used control charts for autocorrelated data based on ARFIMA and AR integrated MA(ARIMA) models to monitor the air quality in Taiwan; they determined that the control chart based on the ARFIMA model is more efficient than that based on the ARIMA model. Rabyk and Schmid [25] suggested the EWMA control chart for detecting changes in the mean of a long-memory process. The control was derived from the results of computations performed on an ARFIMA(p, d, q) process. Meanwhile, the current study focuses on the application of a CUSUM control chart to detect changes in the mean of a long-memory AR fractionally integrated process with an exogenous variable (ARFIX).

In the literature, Monte Carlo simulation, the Markov chain approach, explicit formulas, and integral equations are the primary approaches for computing the ARL. For example, Muhammad [26] and Muhammad *et al.* [27] employed the Monte Carlo simulations to evaluate the ARL on mixed HEWMA and CUSUM control chart for the Weibull distribution.

Brook and Evans [28] used the Markov chain approach to investigate the run length properties of a CUSUM control chart under the assumption of independent and identically distributed (i.i.d.) observations. Hawkins [29] improved the Markov chain approach by using Richardson extrapolation for an entire family of distributions including the Chi-squared distribution. Champ and Rigdon [30] used integral equations to determine the ARL. Fredholm integral equations of the second kind have been employed as part of the NIE approach used to calculate the ARL [31]. Acosta-Mejja *et al.* [32] recently used an integral equation approach for the ARL numerically approximated using the Gauss-Legendre quadrature. Note that the sample variance has a skewed right Chi-squared distribution that is constrained to the half-real line. Knoth [33] proposed utilizing a piecewise collocation method rather than the Gauss-Legendre quadrature to approximate the ARL. Numerical integration (or quadrature) is frequently referred to as a way of approximating the integral. The midpoint rule, the composite trapezoidal rule, the composite Simpson's rule, and the Gaussian rule are all examples of the quadrature that can be used to approximate integral equations. Indeed, approximating the ARL by using the integral equation technique with the midpoint rule is of great importance [34], [35].

In this study, an approximated ARL was computed by using an NIE method via the Gauss-Legendre quadrature for a CUSUM control chart running a long-memory ARFIX process with exponential white noise. The goal of the control chart is to detect changes in the mean of a long-memory ARFIX process with emphasis on exogenous variable X.

The rest of this article is organized as follows. Materials and methods are presented in Section 2. We provide a brief explanation of the CUSUM control chart, EWMA control chart, and long-memory ARFIX(p,d,r) processes with exponential white noise. Moreover, approximated ARL via the NIE method for an ARFIX(p,d,r) process running on a CUSUM control chart is proposed. A comprehensive numerical evaluation, comparison and provides an example of using real data to illustrate the efficacy of the proposed method. The performance comparison of CUSUM and EWMA control chart running an ARFIX(p,d,r) process is presented in Section 3, and some concluding remarks are given in Section 4.

2 Materials and Methods

2.1 *The CUSUM and EWMA control charts and the long-memory ARFIX(p, d, r) model with exponential white noise*

The CUSUM statistic can be obtained from the following recursive Equation (1):

$$C_t = \max\left\{C_{t-1} + Y_t - k,\ 0\right\},\ t = 1,2,\ldots, \tag{1}$$

Where k is a suitably chosen positive constant termed the reference value for the chart and Y_t is the sequence of a long-memory ARFIX(p, d, r) process with exponential white noise. Starting value $C_0 = \psi$, where ψ is the initial value. The EWMA statistic can be written as Equation (2)

$$Z_t = (1-\gamma)Z_{t-1} + \gamma Y_t,\ t = 1,2,\ldots, \tag{2}$$

where $\gamma \in (0,1]$ is a smoothing parameter. The starting value is $Z_0 = Y_0$. The EWMA control chart performs sensitively for small process parameter shifts and small values of γ The upper control limit (UCL), control limit (CL), and lower control limit (LCL) to detect the sequence are respectively given by Equation (3)

$$\begin{aligned} UCL &= \mu_0 + L\sigma\sqrt{\frac{\gamma}{2-\gamma}\left[1-(1-\gamma)^{2t}\right]}, \\ CL &= \mu_0, \\ LCL &= \mu_0 - L\sigma\sqrt{\frac{\gamma}{2-\gamma}\left[1-(1-\gamma)^{2t}\right]}, \end{aligned} \tag{3}$$

where L is the width of the CLs for the EWMA control chart (i.e., it is used to control the in-control ARL) and and μ_0 are σ the process mean and standard deviation, respectively. In practice, ARL_0 is fixed at either 370 or 500.

As mentioned previously, Y_t is the sequence of a long-memory ARFIX(p, d, r) process with exponential white noise. This model can be derived by using the following recursive equation:

$$\phi_p(B)(1-B)^d(Y_t - \mu) = \sum_{i=1}^{r}\omega_i X_{it} + \varepsilon_t, \tag{4}$$

where terms $\phi_p(B) = 1 - \phi_1 B - \phi_2 B^2 - \ldots - \phi_p B^p$ are AR polynomials in backward-shift operator B (i.e.,

$B^q Y_t = Y_{t-q}$ for the q^{th} order), μ is the constant process mean, ε_t is a white noise process assumed to follow exponential distribution $\varepsilon_t \sim Exp(\beta)$, $(1 - B)^d$ is a fractional difference operator subjected to a binomial series expansion [20], [36], and d is the degree of differencing parameter. The values for d are interesting in the context of long-memory processes as they are restricted to the range of (0, 0.5) (i.e., non-integer).

Remark: An ARFIMAX(p, d, q, r) process [36] when $q = 0$ is an AR fractionally integrated process with an exogenous variable denoted as ARFIX(p, d, r), which is the main goal of the present work.

Equation (4) for a general long-memory ARFIX(p, d, r) process with exponential white noise running on a CUSUM control chart can be rewritten as Equation (5)

$$\begin{aligned} Y_t = {} & \mu + \phi_1 Y_{t-1} + \phi_2 Y_{t-2} + \ldots + \phi_p Y_{t-p} \\ & + d(Y_{t-1} - \phi_1 Y_{t-2} - \phi_2 Y_{t-3} - \ldots - \phi_p Y_{t-p-1}) \\ & + \frac{1}{2} d(d-1)(-Y_{t-2} + \phi_1 Y_{t-3} + \phi_2 Y_{t-4} + \ldots + \phi_p Y_{t-p-2}) \\ & + \ldots + \omega_1 X_{1t} + \omega_2 X_{2t} + \ldots + \omega_r X_{rt} + \varepsilon_t \end{aligned} \tag{5}$$

where ϕ_1 is an AR coefficient ($-1 \le \phi_1 \le 1; i = 1, 2, \ldots, p$) and ω_1 are coefficients corresponding to r. The initial value of a long-memory ARFIX(p, d, r) process must satisfy $Y_{t-1}, Y_{t-2}, \ldots, Y_{t-p}, Y_{t-(p+1)}, \ldots, X_{1t}, X_{2t}, \ldots, X_{rt}$, are equal to 1, and the initial value of exponential white noise $\varepsilon_t = 1$

Let τ_h be the stopping time of the CUSUM chart with a predetermined threshold of H given as follows Equation (6)

$$\tau_H = \inf\{ t > 0;\ C_t > H \}, \tag{6}$$

for $H > \psi$ where H is the upper control limit (UCL).

2.2 *The approximate ARL based on the NIE method for a CUSUM control chart*

Here, the ARL is approximated by using the NIE method based on a Fredholm's integral equation of the second kind [31]. As is known, the NIE method can be applied by using the Gauss-Legendre quadrature and numerically computing the integral equation.

Let P_c and E_c denote the probability measure and induced expectation corresponding to the initial value ψ respectively. A process on a CUSUM control chart starts with the initial value ψ and the initial value for monitoring with the CUSUM control chart statistic is $C_0 = \psi$; $0 < \psi < H$. Meanwhile, the function $\ell(\psi)$ denotes the ARL of a long-memory ARFIX(p, d, r) process running on a CUSUM control chart. Thus, $\ell(\psi) = E_c(\tau_H) < \infty$ satisfies the following integral equation:

$$\ell(\psi) = 1 + P_c\{C_1 = 0\}\ell(0) + E_c[I\{0 < C_1 < H\}\ell(C_1)], \tag{7}$$

where C_1 is the first observation for which $I\{0 < C_1 < H\}$ is an indicator function.

Equation (7) is the integral equation for computing the ARL of an upper-sided CUSUM control chart by using a Fredholm integral equation of the second kind [31]. Thereby, $\ell(\psi)$ can be written in the form Equation (8)

$$\begin{aligned} \ell(\psi) = {} & 1 + \ell(0) F(k - \psi - Y_t) \\ & + \int_0^H \ell(u) f(u + k - \psi - \mu - \phi_1 Y_{t-1} - \phi_2 Y_{t-2} - \ldots - \phi_p Y_{t-p} \\ & - d(Y_{t-1} - \phi_1 Y_{t-2} - \phi_2 Y_{t-3} - \ldots - \phi_p Y_{t-p-1}) \\ & - \frac{1}{2} d(d-1)(-Y_{t-2} + \phi_1 Y_{t-3} + \phi_2 Y_{t-4} + \ldots + \phi_p Y_{t-p-2}) \\ & - \ldots - \omega_1 X_{1t} - \omega_2 X_{2t} - \ldots - \omega_r X_{rt} - \varepsilon_t) du, \end{aligned} \tag{8}$$

where $f(.)$ and $F(.)$ are the probability density function (pdf) and cumulative distribution function (cdf) of ε_t respectively, which can both be approximated numerically.

The integral equation in Equation (9) is used as the basis for calculating the ARL obtained by using the method and the analytical formulas in the following subsection.

2.2.1 The approximated ARL by using the NIE method

This is a new approximated ARL by using the NIE method for a CUSUM control chart running a long-memory ARFIX(p, d, r) process with exponential white noise. The conventional Gauss-Legendre quadrature rule technique can be used to approximate the ARL quite accurately

Obtaining numerical solutions can be accomplished by using the Gauss-Legendre quadrature rule technique in Equation (9). Integral $\int_0^H f(u)du$ can be approximated by the sum of the areas of rectangles with bases H / m

and heights chosen as the values of f at the midpoints of intervals with length H / m beginning at zero. Interval $[0, H]$ is divided into partitions $0 \le a_1 \le \ldots \le a_m \le H$, while $w_j = H / m; j = 1, 2, \ldots, m$ are sets of constant weights. The summation form to obtain the approximation for the integral is as follows:

$$\int_0^H W(u) f(u) du \approx \sum_{j=1}^{m} w_j f(a_j),$$

where $W(u)$ is a weight function, and $a_j = \frac{H}{m}\left(j - \frac{1}{2}\right)$.

Function $\ell^{NIE}(\psi)$ provides the approximated ARL by using the NIE method via the Gauss-Legendre quadrature on interval $[0, H]$ The system of linear equations with m unknowns can be transformed into an integral equation. Therefore, the integral equation comprises set $\ell^{NIE}(\psi) = \ell^{NIE}(a_1), \ldots, \ell^{NIE}(a_m)$, which can be approximately derived as

$$\begin{aligned}
\ell^{NIE}(a_1) = \; & 1 + \ell^{NIE}(a_1)\big[F(k - a_1 - \mu - \phi_1 Y_{t-1} - \ldots + \phi_p Y_{t-p} \\
& - d(Y_{t-1} - \phi_1 Y_{t-2} - \ldots - \phi_p Y_{t-p-1}) \\
& - \frac{1}{2} d(d-1)(-Y_{t-2} + \phi_1 Y_{t-3} + \ldots + \phi_p Y_{t-p-2}) \\
& - \ldots - \omega_1 X_{1t} - \ldots - \omega_r X_{rt} - \varepsilon_t \\
& + w_1 f(k - \mu - \phi_1 Y_{t-1} - \ldots + \phi_p Y_{t-p} \\
& - d(Y_{t-1} - \phi_1 Y_{t-2} - \ldots - \phi_p Y_{t-p-1}) \\
& - \frac{1}{2} d(d-1)(-Y_{t-2} + \phi_1 Y_{t-3} + \ldots + \phi_p Y_{t-p-2}) \\
& - \ldots - \omega_1 X_{1t} - \ldots - \omega_r X_{rt} - \varepsilon_t)\big] \\
& + \sum_{j=2}^{m} w_j \ell^{NIE}(a_j) f(a_j + k - a_1 - \mu - \phi_1 Y_{t-1} \\
& - \ldots + \phi_p Y_{t-p} - d(Y_{t-1} - \phi_1 Y_{t-2} - \ldots - \phi_p Y_{t-p-1}) \\
& - \frac{1}{2} d(d-1)(-Y_{t-2} + \phi_1 Y_{t-3} + \ldots + \phi_p Y_{t-p-2}) \\
& - \ldots - \omega_1 X_{1t} - \ldots - \omega_r X_{rt} - \varepsilon_t), \\
\vdots \qquad & \qquad \vdots \\
\ell^{NIE}(a_m) = \; & 1 + \ell^{NIE}(a_1)\big[F(k - a_m - \mu - \phi_1 Y_{t-1} - \ldots + \phi_p Y_{t-p} \\
& - d(Y_{t-1} - \phi_1 Y_{t-2} - \ldots - \phi_p Y_{t-p-1}) \\
& - \frac{1}{2} d(d-1)(-Y_{t-2} + \phi_1 Y_{t-3} + \ldots + \phi_p Y_{t-p-2}) \\
& - \ldots - \omega_1 X_{1t} - \ldots - \omega_r X_{rt} - \varepsilon_t \\
& + w_1 f(a_1 + k - a_m - \mu - \phi_1 Y_{t-1} - \ldots + \phi_p Y_{t-p} \\
& - d(Y_{t-1} - \phi_1 Y_{t-2} - \ldots - \phi_p Y_{t-p-1}) \\
& - \frac{1}{2} d(d-1)(-Y_{t-2} + \phi_1 Y_{t-3} + \ldots + \phi_p Y_{t-p-2}) \\
& - \ldots - \omega_1 X_{1t} - \ldots - \omega_r X_{rt} - \varepsilon_t)\big] \\
& + \sum_{j=2}^{m} w_j \ell^{NIE}(a_j) f(a_j + k - a_m - \mu - \phi_1 Y_{t-1} \\
& - \ldots + \phi_p Y_{t-p} - d(Y_{t-1} - \phi_1 Y_{t-2} - \ldots - \phi_p Y_{t-p-1}) \\
& - \frac{1}{2} d(d-1)(-Y_{t-2} + \phi_1 Y_{t-3} + \ldots + \phi_p Y_{t-p-2}) \\
& - \ldots - \omega_1 X_{1t} - \ldots - \omega_r X_{rt} - \varepsilon_t),
\end{aligned}$$

This can be rewritten in matrix form as

$$\mathbf{L}_{m\times 1} = \mathbf{1}_{m\times 1} + \mathbf{R}_{m\times m}\mathbf{L}_{m\times 1}, \tag{9}$$

where $\mathbf{L}_{m\times 1} = \left[\ell^{NIE}(a_1), \ell^{NIE}(a_2), \ldots, \ell^{NIE}(a_m)\right]'$, $\mathbf{1}_{m\times 1} = [1, 1, \ldots, 1]'$ is a column vector of $\ell^{NIE}(a_j)$ and ones, and $\mathbf{R}_{m\times m}$ is a matrix with dimensions $m \times m$ written as

$$\mathbf{R}_{m\times m} = \begin{bmatrix} r_{11} & r_{12} & \cdots & r_{1m} \\ r_{21} & r_{22} & \cdots & r_{2m} \\ \vdots & \vdots & \ddots & \vdots \\ r_{m1} & r_{m2} & \cdots & r_{mm} \end{bmatrix},$$

for

$$\begin{aligned}
r_{ij} = \; & F(k - a_i - \mu - \phi_1 Y_{t-1} - \ldots + \phi_p Y_{t-p} \\
& - d(Y_{t-1} - \phi_1 Y_{t-2} - \ldots - \phi_p Y_{t-p-1}) \\
& - \frac{1}{2} d(d-1)(-Y_{t-2} + \phi_1 Y_{t-3} + \ldots + \phi_p Y_{t-p-2}) \\
& - \ldots - \omega_1 X_{1t} - \ldots - \omega_r X_{rt} - \varepsilon_t) \\
& + w_j f(a_j + k - a_i - \mu - \phi_1 Y_{t-1} - \ldots + \phi_p Y_{t-p} \\
& - d(Y_{t-1} - \phi_1 Y_{t-2} - \ldots - \phi_p Y_{t-p-1}) \\
& - \frac{1}{2} d(d-1)(-Y_{t-2} + \phi_1 Y_{t-3} + \ldots + \phi_p Y_{t-p-2}) \\
& - \ldots - \omega_1 X_{1t} - \ldots - \omega_r X_{rt} - \varepsilon_t),
\end{aligned}$$

where $i, j = 1, 2, \ldots, m$. The matrix form in Equation (10) can be reformatted equivalently as

$$(\mathbf{I}_m - \mathbf{R}_{m\times m})\mathbf{L}_{m\times 1} = \mathbf{1}_{m\times 1},$$

where $\mathbf{I}_m = diag(1, 1, \ldots, 1)$ is unit matrix order m. If $(\mathbf{I}_m - \mathbf{R}_{m\times m})$ is invertible and exists, then the approximated ARL via the NIE method for the integral equations in the matrix is provided as follows:

$$\mathbf{L}_{m\times 1} = (\mathbf{I}_m - \mathbf{R}_{m\times m})^{-1}\mathbf{1}_{m\times 1}, \tag{10}$$

where $\mathbf{L}_{m\times 1} = [\ell^{NIE}(a_1), \ell^{NIE}(a_2), ..., \ell^{NIE}(a_m)]'$ after computing $\ell^{NIE}(a_1)$, $\ell^{NIE}(a_2)$, ..., $\ell^{NIE}(a_m)$, and replacing a_i by ψ, respectively.

Hence, the approximated ARL via the NIE derived by using the Gauss-Legendre quadrature rule on a CUSUM control chart can be expressed as

$$\begin{aligned}\ell^{NIE}(\psi) = 1 + \ell^{NIE}(a_1)F(&k - \psi - \mu - \phi_1 Y_{t-1} - ... + \phi_p Y_{t-p} \\ &- d(Y_{t-1} - \phi_1 Y_{t-2} - ... - \phi_p Y_{t-p-1}) \\ &- \frac{1}{2}d(d-1)(-Y_{t-2} + \phi_1 Y_{t-3} + ... + \phi_p Y_{t-p-2}) \\ &- ... - \omega_1 X_{1t} - ... - \omega_r X_{rt} - \varepsilon_t) \\ &+ \sum_{j=1}^{m} w_j \ell^{NIE}(a_j) f(a_j + k - \psi - \mu - \phi_1 Y_{t-1} \\ &- ... + \phi_p Y_{t-p} - d(Y_{t-1} - \phi_1 Y_{t-2} - ... - \phi_p Y_{t-p-1}) \\ &- \frac{1}{2}d(d-1)(-Y_{t-2} + \phi_1 Y_{t-3} + ... + \phi_p Y_{t-p-2}) \\ &- ... - \omega_1 X_{1t} - ... - \omega_r X_{rt} - \varepsilon_t),\end{aligned} \quad (11)$$

with $w_j = \frac{H}{m}$, and $a_j = \frac{H}{m}\left(j - \frac{1}{2}\right)$; $j = 1, 2, \ldots, m$.

2.2.2 The analytical ARL by using explicit formulas

The analytical ARL derived using explicit formulas for a process running on a CUSUM control chart can be written as

$$\ell^{EF}(\psi) = e^{\lambda H}(1 - \lambda H) + e^{\lambda\left(\begin{matrix} k-(\mu+\phi_1 Y_{t-1}+\phi_2 Y_{t-2}+... \\ +d(Y_{t-1}-...-\phi_p Y_{t-p-1}) \\ +\frac{1}{2}d(d-1)(-Y_{t-2}+... \\ +\phi_p Y_{t-p-2})+...,+\omega_1 X_{1t}+...+\varepsilon_t) \end{matrix}\right) + \lambda H} - e^{\lambda\psi},$$

where $\ell^{EF}(\psi)$ is used for the in-control ARL (ARL_0) process and detecting changes in the process mean (ARL_1). It can be written as

$$\ell^{EF}(\psi) = \begin{cases} e^{\lambda_0 H}(1 - \lambda_0 H) + e^{\lambda_0\left(\begin{matrix} k-(\mu+\phi_1 Y_{t-1}+\phi_2 Y_{t-2}+... \\ +d(Y_{t-1}-...-\phi_p Y_{t-p-1}) \\ +\frac{1}{2}d(d-1)(-Y_{t-2}+... \\ +\phi_p Y_{t-p-2})+...,+\omega_1 X_{1t}+...+\varepsilon_t) \end{matrix}\right) + \lambda_0 H} - e^{\lambda_0\psi}, \\ e^{\lambda_1 H}(1 - \lambda_1 H) + e^{\lambda_1\left(\begin{matrix} k-(\mu+\phi_1 Y_{t-1}+\phi_2 Y_{t-2}+... \\ +d(Y_{t-1}-...-\phi_p Y_{t-p-1}) \\ +\frac{1}{2}d(d-1)(-Y_{t-2}+... \\ +\phi_p Y_{t-p-2})+...,+\omega_1 X_{1t}+...+\varepsilon_t) \end{matrix}\right) + \lambda_1 H} - e^{\lambda_1\psi}, \end{cases} \quad (12)$$

3 Results and Discussion

For a long-memory ARFIX(p, d, r) process, we assumed that the white noise is exponentially distributed where the mean parameter of the exponential is β for ARFIX(p = 1, d = 0.2, r = 1) running on a CUSUM control chart for k = 3.0, 3.5, or 4.0, the values of H were calculated by using Equation (11) or (12) as H = 3.96709, 3.26334, and 2.67966, respectively (Table 1). Consequently, each combination of (k, H) was used in computations for ARL_0 = 370 or 500. Moreover, $\lambda = \lambda_0 = 1$ for the in-control ARL process while $\lambda_1 = (1 + \delta)\lambda_0$ for out-of-control process, for $0 < \delta < 1$. For the out-of-control process, the shift size (δ) was set as δ = 0.01, 0.03, 0.05, 0.07, 0.10, 0.30, 0.50, 1.00, 2.00, or 4.00. The out-of-control performance results for the CUSUM control chart running a long-memory ARFIX(p, d, r) process with exponential white noise are given in Tables 2 and 3. These results are approximated via Equation (11) by using the Gauss-Legendre quadrature rule with the number of division points m = 800 nodes by solving the system of linear equations.

3.1 *Comparison of the approximated and analytical ARLs for a long-memory ARFIX(p, d, r) process with exponential white noise running on a CUSUM control chart*

The performance comparison is expressed by calculating the relative percentage change (r%) as follows:

$$(r\%) = \left| \frac{\ell^{EF}(\psi) - \ell^{NIE}(\psi)}{\ell^{EF}(\psi)} \right| \times 100\%,$$

where $\ell^{NIE}(\psi)$ and $\ell^{EF}(\psi)$ are the predefined ARL_0 = 370 or 500 approximated via the NIE method and derived by using the explicit formulas, respectively.

The values of CL (H) on a CUSUM control chart for k = 3.0, 3.5, or 4.0, and coefficient parameters ϕ_1 = 0.10, ϕ_2 = 0.20, ϕ_3 = 0.30, and ω_1 = 0.20 for ARL_0 = 370 or 500 are reported in Table 1. It was found that as k increases, H decreases on the CUSUM control chart for all of the long-memory ARFIX(p ,0.2, 1) models. When p was changed from 1 to 3, the findings indicate that p increased and H increased for each value of k.

Table 1: The values of CL H of the CUSUM chart in the zero-state case for ARL_0 = 370 or 500, λ = 1, and k = 3.0, 3.5, or 4.0

ARFIX(*p*, 0.2, 1)	Coefficient Parameters				ARL_0	k		
	ϕ_1	ϕ_2	ϕ_3	ω_1		3.0	3.5	4.0
p = 1	0.1	-	-	0.3	370	3.967090	3.263340	2.6796600
					500	4.317200	3.585383	2.9911290
p = 2	0.1	0.2	-	0.3	370	4.205980	3.435022	2.8303901
					500	4.573657	3.761815	3.1439600
p = 3	0.1	0.2	0.3	0.3	370	4.670457	3.713077	3.0641010
					500	5.101390	4.050036	3.3817230

Table 2: Comparison of the ARLs obtained by using the NIE method and explicit formulas for a long-memory ARFIX(*p*, 0.2, 1) process running on a CUSUM control chart when ARL_0 = 370

ARFIX (*p*, 0.2, 1)	k	ARL	λ_1									
			1.01	1.03	1.05	1.07	1.10	1.30	1.50	2.00	3.00	5.00
p = 1	3.0	$\ell^{NIE}(\psi)$	345.444	303.592	268.131	237.922	200.516	78.869	40.300	14.204	5.483	2.740
		$\ell^{EF}(\psi)$	346.186	304.224	268.672	238.388	200.891	78.980	40.343	14.213	5.485	2.741
		r%	0.21	0.21	0.20	0.20	0.19	0.14	0.11	0.06	0.04	0.04
	3.5	$\ell^{NIE}(\psi)$	346.888	307.171	273.246	244.119	207.720	85.601	44.786	15.893	5.901	2.811
		$\ell^{EF}(\psi)$	347.544	307.737	273.737	244.548	208.072	85.717	44.835	15.904	5.903	2.811
		r%	0.19	0.18	0.18	0.18	0.17	0.14	0.11	0.07	0.03	0.00
	4.0	$\ell^{NIE}(\psi)$	347.638	308.950	275.782	247.205	211.340	89.230	47.348	16.973	6.214	2.881
		$\ell^{EF}(\psi)$	348.193	309.432	276.204	247.575	211.645	89.331	47.394	16.984	6.216	2.882
		r%	0.16	0.16	0.15	0.15	0.14	0.11	0.10	0.06	0.03	0.03
p = 2	3.0	$\ell^{NIE}(\psi)$	344.762	301.880	265.691	234.980	197.126	75.875	38.399	13.555	5.347	2.726
		$\ell^{EF}(\psi)$	345.518	302.519	266.235	235.445	197.497	75.979	38.438	13.562	5.348	2.727
		r%	0.22	0.21	0.20	0.20	0.19	0.14	0.10	0.05	0.02	0.04
	3.5	$\ell^{NIE}(\psi)$	346.596	306.463	272.235	242.893	206.288	84.218	43.838	15.516	5.800	2.791
		$\ell^{EF}(\psi)$	347.278	307.049	272.743	243.335	206.649	84.335	43.887	15.527	5.802	2.792
		r%	0.20	0.19	0.19	0.18	0.17	0.14	0.11	0.07	0.03	0.04
	4.0	$\ell^{NIE}(\psi)$	347.474	308.571	275.243	246.549	210.569	88.436	46.779	16.724	6.139	2.863
		$\ell^{EF}(\psi)$	348.057	309.076	275.684	246.935	210.887	88.545	46.826	16.735	6.141	2.864
		r%	0.17	0.16	0.16	0.16	0.15	0.12	0.10	0.07	0.03	0.03
p = 3	3.0	$\ell^{NIE}(\psi)$	343.059	297.542	259.522	227.575	188.658	68.769	34.077	12.203	5.107	2.719
		$\ell^{EF}(\psi)$	343.805	298.159	260.035	228.004	188.989	68.843	34.100	12.206	5.107	2.719
		r%	0.22	0.21	0.20	0.19	0.18	0.11	0.07	0.02	0.00	0.00
	3.5	$\ell^{NIE}(\psi)$	346.045	305.103	270.291	240.536	203.545	81.634	42.105	14.856	5.634	2.762
		$\ell^{EF}(\psi)$	346.762	305.718	270.821	240.994	203.917	81.749	42.152	14.866	5.636	2.763
		r%	0.21	0.20	0.20	0.19	0.18	0.14	0.11	0.07	0.04	0.04
	4.0	$\ell^{NIE}(\psi)$	347.181	307.877	274.255	245.346	209.156	87.016	45.771	16.296	6.014	2.835
		$\ell^{EF}(\psi)$	347.805	308.417	274.724	245.757	209.494	87.129	45.819	16.308	6.016	2.835
		r%	0.18	0.18	0.17	0.17	0.16	0.13	0.10	0.07	0.03	0.00

Table 3: Comparison of the ARLs obtained by using the NIE method and explicit formulas for a long-memory ARFIX(p, 0.2, 1) process running on a CUSUM control chart when ARL_0 = 500

ARFIX (p, 0.2, 1)	k	ARL	λ_1									
			1.01	1.03	1.05	1.07	1.10	1.30	1.50	2.00	3.00	5.00
$p=1$	3.0	$\ell^{NIE}(\psi)$	464.737	405.057	354.893	312.488	260.462	96.456	47.258	15.722	5.843	2.862
		$\ell^{EF}(\psi)$	465.827	405.976	355.672	313.153	260.99	96.601	47.311	15.732	5.844	2.862
		r%	0.23	0.23	0.22	0.21	0.20	0.15	0.11	0.06	0.02	0.00
	3.5	$\ell^{NIE}(\psi)$	467.003	410.672	362.879	322.113	271.559	106.356	53.63	17.93	6.373	2.947
		$\ell^{EF}(\psi)$	467.967	411.506	363.598	322.735	272.065	106.513	53.695	18.003	6.375	2.948
		r%	0.21	0.20	0.20	0.19	0.19	0.15	0.12	0.41	0.03	0.03
	4.0	$\ell^{NIE}(\psi)$	468.145	413.385	366.732	326.777	276.989	111.561	57.194	19.415	6.765	3.031
		$\ell^{EF}(\psi)$	468.981	414.107	367.358	327.322	277.436	111.708	57.256	19.429	6.768	3.031
		r%	0.18	0.17	0.17	0.17	0.16	0.13	0.11	0.07	0.04	0.00
$p=2$	3.0	$\ell^{NIE}(\psi)$	463.604	402.229	350.887	307.689	254.981	91.852	44.440	14.815	5.663	2.844
		$\ell^{EF}(\psi)$	464.713	403.155	351.665	308.347	255.497	91.982	44.485	14.822	5.664	2.844
		r%	0.24	0.23	0.22	0.21	0.20	0.14	0.10	0.05	0.02	0.00
	3.5	$\ell^{NIE}(\psi)$	466.558	409.586	361.335	320.247	269.397	104.357	52.305	17.491	6.247	2.924
		$\ell^{EF}(\psi)$	467.566	410.447	362.075	320.886	269.914	104.514	52.368	17.504	6.249	2.924
		r%	0.22	0.21	0.20	0.20	0.19	0.15	0.12	0.07	0.03	0.00
	4.0	$\ell^{NIE}(\psi)$	467.896	412.808	365.914	325.787	275.834	110.428	56.403	19.087	6.67	3.009
		$\ell^{EF}(\psi)$	468.769	413.561	366.566	326.354	276.298	110.579	56.466	19.101	6.673	3.01
		r%	0.19	0.18	0.18	0.17	0.17	0.14	0.11	0.07	0.04	0.03
$p=3$	3.0	$\ell^{NIE}(\psi)$	460.48	394.321	339.721	294.38	239.915	79.897	37.464	12.776	5.325	2.835
		$\ell^{EF}(\psi)$	461.562	395.194	340.429	294.959	240.347	79.973	37.481	12.776	5.325	2.835
		r%	0.23	0.22	0.21	0.20	0.18	0.10	0.05	0.00	0.00	0.00
	3.5	$\ell^{NIE}(\psi)$	465.698	407.466	358.32	316.612	265.199	100.58	49.857	16.608	6.036	2.889
		$\ell^{EF}(\psi)$	466.755	408.364	359.087	317.269	265.729	100.734	49.917	16.62	6.038	2.889
		r%	0.23	0.22	0.21	0.21	0.20	0.15	0.12	0.07	0.03	0.00
	4.0	$\ell^{NIE}(\psi)$	467.452	411.753	364.416	323.972	273.719	108.391	55.003	18.523	6.514	2.975
		$\ell^{EF}(\psi)$	468.381	412.551	365.105	324.571	274.207	108.546	55.067	18.537	6.516	2.977
		r%	0.20	0.19	0.19	0.18	0.18	0.14	0.12	0.08	0.03	0.07

The numerical results for approximated ARL obtained via the NIE method and analytical ARL by using explicit formulas for the out-of-control ARL for detecting changes in the process mean ($\lambda_1 > \lambda_0$) are reported in Tables 2 and 3. The results indicate that the ARLs derived by using the NIE method and explicit formulas tended to decrease more rapidly as the magnitude of the process mean change (λ_1) increases, the decreasing order being long-memory process models ARFIX($p=1$, 0.2, 1), ARFIX($p=2$, 0.2, 1) and ARFIX(p = 3, 0.2, 1) Bearing in mind that a good performance of the CUSUM control chart requires the ARL_1 value to be as small as possible, we observed that for long-memory ARFIX(p, 0.2, 1) processes, ARL_1 reduces rapidly for a small process mean change ($1.01 \le \lambda_1 < 1.10$) and continues to do so for a moderate process mean change ($1.10 \le \lambda_1 < 5.00$). Moreover, the performances with the ARFIX($p=3$, 0.2, 1) model were lower than with ARFIX($p=2$, 0.2, 1) and ARFIX(p = 1, 0.2, 1) for each reference parameter (k) level (Table 2 for ARL_0 = 370 and Table 3 for ARL_0 = 500). Moreover, the associated reference value is inversely proportional to H and directly proportional to the out-of-control ARL (ARL_1) obtained by using both methods. In addition, for $ARL_0 = 370$ or 500, when comparing the ARL_1 values for $k = 3.0$, 3.5, or 4.0 the model with the lowest k value most quickly detected a change in the process mean. The percentage change (r%) results calculated at various magnitudes of process mean changes for the three long-memory ARFIX(p, 0.2, 1) processes were less than 0.25, indicating that the proposed method is very accurate and in excellent agreement with the explicit formulas approach.

The summary of the NIE method is based on the results for evaluation of ARL and comparison between approximated ARL and analytical ARL for monitoring the mean of a long-memory ARFIX running on a CUSUM control chart. The solution of the integral equation can be approximated ARL using of Gauss-Legendre quadrature rule [30]. The results show that the NIE method is an easier alternative to ARL calculations which represent the accuracy of the ARL [34], [35]. However, the Gauss-Legendre rule provided the simplest ARL calculation and achieved the highest accuracy for the given number of nodes. In the case of a large number of nodes, analytical ARL derived using explicit formulas is an alternative for the evaluation of ARL [36]–[38].

3.2 *An example using real data on a CUSUM control chart to monitor changes in the process mean*

This subsection presents real data using the NIE method on a CUSUM control chart to monitor changes in the process mean were applied to two types of data. The first example was a real dataset of Mutual Fund: K Positive Change Equality Fund - A(A) (abbreviation K-CHANGE-A(A)) for the Kasikorn bank in Thailand with the exogenous variable being the exchange rate and the second one is the data were taken from the commodity market of gold futures price with the exogenous variable being the exchange rate is used to illustrate the CUSUM control chart's efficacy.

Example 1: The dataset represents K-CHANGE-A(A) (source: https:// kasikornasset.com/TH/mutual-fund/fund-template/Pages/K-CHANGE-A(A).aspx) with the exogenous variable being the exchange rate for USD/THB (source: https://th.investing.com/currencies/usd-thb-historical-data) consisted of 161 observations collected daily (5 days per week) from 20 November 2020 to 6 August 2021.

Example 2: The dataset is given by the commodity market of gold futures price (source: https://th.investing.com/commodities/gold) with the exogenous variable being the exchange rate for USD/THB. This dataset contains 146 observations collected daily (5 days per week) for the period of 23 June 2020 to 13 January 2021.

For modeling purposes, the Eviews 10 statistical software package was used to filter and estimate the model parameters. Significant p-values for the best-fitting long-memory ARFIX(p, d, r) process are shown in Table 4.

Table 4: ARFIX(p, d, r) model fitting for the example dataset 1 and 2 with the exogenous variable as the exchange rate of USD/THB dataset

Example	Variable	Coefficient	Std. Error	t-Statistic	Prob.
1	USD	0.676247	0.035190	19.21720	0.0000
	d	0.221642	0.107682	2.058290	0.0412
	AR(1)	0.937123	0.053237	17.60269	0.0000
2	USD	–108.1627	19.86484	–5.444932	0.0000
	d	0.499999	6.57E-10	7.61E+08	0.0000
	AR(1)	0.475489	0.082231	5.782335	0.0000
	AR(2)	0.297705	0.081395	3.657533	0.0004

The results in Table 4 reveal that the probability for variable X was significant (0.05; p-value = 0.0000), which indicates that the exchange rate does impact the Mutual Fund for K-CHANGE-A(A) and the commodity market of gold futures price. It can also be seen that the dataset 1 is suitable for a long-memory ARFIX(1, 0.221642, 1) process by presenting statistically significant parameters with coefficients $\phi_1 = 0.937123$, $\omega_1 = 0.676247$. Likewise dataset 2 is suitable for a long-memory ARFIX(1, 0.499999, 1) process by presenting statistically significant parameters with coefficients $\phi_1 = 0.475489$, $\phi_2 = 0.297705$, $\omega_1 = 108.1627$ and the residual series behaving as white noise.

Table 5 reports the results of testing whether the distribution of the white noise is exponential according to the Kolmogorov-Smirnov test by using the SPSS software package. In the null hypothesis test, the white noise was found to be significantly exponentially distributed (p-value > 0.05) with a mean of 0.2193 and 14.5106 for dataset 1 and 2, respectively when the process was in-control.

Table 5: Testing the distribution of the white noise for the example dataset 1 and 2 with the exogenous variable as the USD/THB exchange rate dataset

Example	Alternative Hypothesis: Two-Sided		
	Exponential Parameter	One-Sample Kolmogorov-Smirnov Test	Asymptotic Significance (2-Sided)
1	0.2193	1.289	0.072*
2	14.5106	0.986	0.286*

According to the results in Tables 4 and 5, the long-memory ARFIX(*p, d, r*) process consists of the following equations:

This dataset 1 demonstrates the long-memory ARFIX(1, 0.221642, 1) process is

$$Y_t = \phi_1 Y_{t-1} - 0.221642(Y_{t-1} + \phi_1 Y_{t-2}) + 0.086258(Y_{t-2} - \phi_1 Y_{t-3}) \\ +0.05113278(Y_{t-3} - \phi_1 Y_{t-4}) + 0.676247 X_t + \xi_t$$

where $\xi_t \sim Exp(\lambda_0 = 0.2193)$.

The dataset 2 represent long-memory ARFIX(2, 0.499999, 1) process is

$$Y_t = \phi_1 Y_{t-1} + \phi_2 Y_{t-2} + 0.499999(Y_{t-1} - \phi_1 Y_{t-2} - \phi_2 Y_{t-3}) \\ +0.12499(Y_{t-2} - \phi_1 Y_{t-3} - \phi_2 Y_{t-4}) \\ +0.06250(Y_{t-3} - \phi_1 Y_{t-4} - \phi_2 Y_{t-5}) \\ -108.1627 X_t + \xi_t$$

where $\xi_t \sim Exp(\lambda_0 = 14.5106)$.

3.3 *Performance comparison of CUSUM and EWMA control chart running an ARFIX(p, d, r) process*

Here, the approximated NIE of the CUSUM control chart is compared with that of the EWMA control chart. The approximated ARLs of the CUSUM and EWMA control charts can both be obtained by using the NIE method. For the CUSUM control chart, when $k = 3.0$ the desired ARL_0 is set as 370 and $H = 0.487876$ and 25.71797 are computed for long-memory ARFIX(1, 0.221642, 1) and ARFIX(2, 0.499999, 1) processes, respectively. The results summarized in Table 6 for the ARL obtained with the NIE method for a CUSUM control chart are clearly consistent with those in Tables 2 and 3.

The numerical results were obtained from the method for all cases when detecting small-to-moderate-sized changed in the process mean. The smoothing parameter for the EWMA control chart is $\gamma \in (0, 1]$, [3], with the recommended value being $0.05 \le \gamma \le 0.25$. In this study, $\gamma = 0.05$ for dataset 1 and $\gamma = 0.07$ for dataset 2 were selected for the corresponding control limits of the EWMA control chart for the desired ARL_0. For simplicity, ARL_0 was set as 370. The method to compute the approximated ARL for the EWMA control chart is similar to that of Sunthornwat *et al.* [38]. The ARL_1 values for the CUSUM and EWMA control charts for the process mean shift values (δ) varying from 0.01 to 1.00 are reported in Table 6. It is noteworthy that, the first example on upper-sided CUSUM control chart when $k = 3.0$ is relatively effective for shifts $\delta = 0.07$–1.00. For instance, when $k = 3.0$ and $\delta = 0.07$, the $ARL_1 = 71.823$ of the upper-sided CUSUM control chart is smaller than the $ARL_1 = 71.929$ of the EWMA control chart when $\gamma = 0.05$. Irrespective of the value of δ the ARL_1 values of the upper-sided CUSUM control chart were generally smaller than the ones of the upper-sided EWMA control chart, especially for moderate shifts ($\delta = 0.07$–1.00). Example 2, the upper-sided CUSUM control chart when $k = 3.0$ is relatively effective for shifts $\delta = 0.50$–1.00. The results reveal that of proposed approximated ARL via the NIE method for a CUSUM control chart is very accurate for moderate shifts.

Table 6: Comparisons of ARLs obtained using the NIE method for both the CUSUM and EWMA control charts running ARFIX Long Memory (1, 0.221642, 1) and ARFIX(2, 0.499999, 1) are derived from the example 1 and 2, respectively, where $ARL_0 = 370$

Example	Control Chart	Parameters	Shift Sizes (δ)							
			0.01	0.03	0.05	0.07	0.10	0.30	0.50	1.00
1	CUSUM	k = 3.0, H = 0.487876	276.630	165.061	105.796	71.823	43.768	6.819	3.174	1.656
	EWMA	$\gamma = 0.05$, $L = 0.0147306$	276.420	164.885	105.776	71.929	43.980	6.970	3.234	1.656
2	CUSUM	k = 3.0, $H = 25.71797$	368.407	365.249	362.126	359.038	354.470	325.876	300.228	246.755
	EWMA	$\gamma = 0.07$, $L = 1.9098$	368.406	365.248	362.124	359.035	354.466	325.875	300.244	246.849

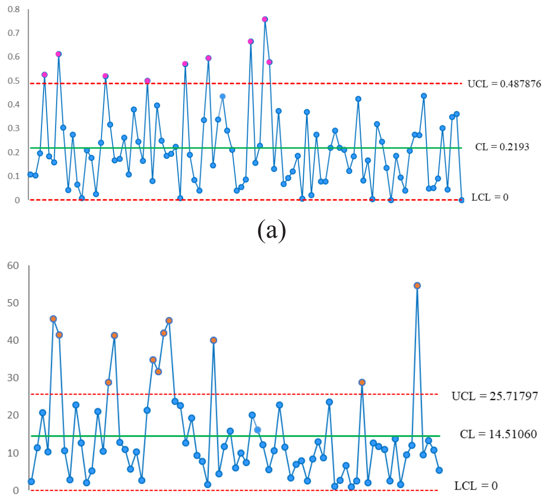

(a)

(b)

Figure 1: Shifts in the mean running on an upper-sided CUSUM control chart for ARL_0 = 370 of (a) long-memory ARFIX(1, 0.221642, 1) process and (b) long-memory ARFIX(2, 0.499999, 1) process.

For ARL_0 = 370 on an upper-sided CUSUM control charts in Figure 1(a), the center line and the lower and upper control limits of the CUSUM control chart were LCL = 0, CL = 0.2193, UCL = 0.487876. The in-control ARL values are plotted as blue points while the red points are the out-of-control values and the red dashed lines indicate the UCL and LCL. The first out-of-control signal occurs at the 4th point and there are 9 out-of-control points altogether. Moreover, Figure 1(b) for long-memory ARFIX(2, 0.499999, 1) process of the CUSUM control chart was LCL = 0, CL = 14.5106, UCL = 25.71797. The first out-of-control signal occurs at the 5th point and there are 11out-of-control points altogether. These results confirm that the proposed NIE method is sensitive to changes in the process mean and is as good at detecting them as the analytical ARL based on explicit formulas.

4 Conclusions

First, the theoretical computation was successfully derived a method for approximating the ARL for a long-memory ARFIX process running on a CUSUM control chart. The approximated ARL obtained by using the NIE method performed well and offers a new approach for validating ARL computation for long-memory scenarios. In addition, the results from the experiment using a two real datasets were similar to those of the theoretical computation. For instance, the excellent efficacy of the method was illustrated by using mutual fund K-CHANGE-A(A) data and the commodity market of gold futures price with the USD/THB exchange rate as the exogenous variable. When comparing the method for CUSUM and EWMA control charts, it was found that it performed better on the former than the latter for moderate shifts in the process mean. Thus, we recommended that the NIE method as a good alternative for the approximate ARL of the CUSUM control chart. It has real-life applications for varieties of data processes, such as finance, economic, hydrology, biology, engineering, social sciences, and environmental. If the data comes from a complex process or an unstable environment [39], these issues should be addressed in future research. Future research could compare the results of the ARL for the CUSUM control chart using the neutrosophic statistical method, such as NCUSUM control chart [39]. The application and implementation of the NCUSUM control chart are provided interesting properties compared to the classical CUSUM control chart. In addition, to extend its practical usage, the methodology could be extended to monitor the process variance and for other distributions of white noise.

Acknowledgement

The author would like to express her gratitude to the Faculty of Applied Science, King Mongkut's University of Technology North Bangkok, Thailand for support with research grant No. 652113.

References

[1] E. S. Page, "Continuous inspection schemes," *Biometrika*, vol. 41, no. 1–2, pp. 100–115, 1954.
[2] S. W. Robert, "Control chart test based on geometric moving averages," *Technometrics*, vol. 1, pp. 239–250, 1959.
[3] D. C. Montgomery, *Introduction to Statistical Quality Control*, 6th ed. New York: John Wiley & Sons, 2009.
[4] M. Riaz, S. A. Abbasi, S. Ahmad, and B. Zaman, "On efficient phase II process monitoring charts," *The International Journal of Advanced*

Manufacturing Technology, vol. 70, pp. 2263–2274, 2014.
[5] R. A. Johnson and M. Bagshaw, "The effect of serial correlation on the performance of CUSUM tests," *Technometrics*, vol. 16, no. 1, pp. 103–112, 1974.
[6] C. W. Lu and M. R. J. Reynolds, "CUSUM charts for monitoring an autocorrelated process," *Journal of Quality Technology*, vol. 33, no. 3, pp. 316–334, 2001.
[7] S. H. Kim, C. Alexopoulos, K. L. Tsui, and J. R. Wilson, "A distribution-free tabular CUSUM chart for autocorrelated data," *IIE Transactions*, vol. 39, no. 3, pp. 317–330, 2007.
[8] W. Jiang, "Average run length computation of ARMA charts for stationary process," *Communications in Statistics*, vol. 30, no. 3, pp. 699–717, 2001.
[9] C. W. Lu and M. R. Reynolds, "EWMA control charts for monitoring the mean of autocorrelated process," *Journal of Quality Technology*, vol. 31, pp. 166–188, 1999.
[10] S. Yue and P. Pilon, "Interaction between deterministic trend and autoregressive process," *Water Resources Research*, vol. 39, no. 4, 2003, doi: 10.1029/2001WR001210.
[11] K. H. Hamed, "Enhancing the effectiveness of prewhitening in trend analysis of hydrologic data," *Journal of Hydrology*, vol. 368, no. 1, pp. 143–155, 2009.
[12] A. D. Karaoglan and G. M. Bayhan, "ARL performance of residual control charts for trend AR(1) process: A case study on peroxide values of stored vegetable oil," *Scientific Research and Essays*, vol. 7, no. 13, pp. 1405–1414, 2012.
[13] R. Zhang and S. Ling, "Asymptotic inference for AR models with heavy-tailed G-GARCH noises," *Econometric Theory*, vol. 31, no. 4, pp. 880–890, 2015.
[14] M. Novkovic, "On exponential autoregressive time series models," *Journal of Mathematics*, vol. 29, no. 1, pp. 97–101, 1999.
[15] M. Ibazizen and H. Fellag, "Bayesian estimation of an AR(1) process with exponential white noise," *Statistics*, vol. 37, no. 5, pp. 365–372, 2003.
[16] I. M. S. Pereira and M. A. Amaral-Turkman, "Bayesian prediction in threshold autoregressive models with exponential white noise," *Sociedad de Estadística e Investigación Operativa*, vol. 13, no. 1, pp. 45–64, 2004.
[17] L. Larbi and H. Fellag, "Robust bayesian analysis of an autoregressive model with exponential innovations," *Afrika Statistika*, vol. 11, no. 1, pp. 955–964, 2016.
[18] S. Suparman, "A new estimation procedure using a reversible jump MCMC algorithm for AR models of exponential white noise," *International Journal of GEOMATE*, vol.15, no. 49, pp. 85–91, 2018.
[19] C. W. J. Granger and R. Joyeux, "An introduction to long memory time series models and fractional differencing." *Journal of Time Series Analysis*, vol. 1, no. 1, pp. 15–29, 1980.
[20] J. R. M. Hosking, "Fractional differencing," *Biometrika*, vol. 68, no. 1, pp. 165–176, 1981.
[21] H. Ebens, "Realized stock index volatility," Ph.D. dissertation, Department of Economics, Johns Hopkins University, USA,1999.
[22] R. Ramjee, "Qualitycontrol charts and persistent processes," Ph.D. dissertation, Department of Mathematical Sciences, Stevens Institute of Technology, USA, 2000.
[23] R. Ramjee, N. Crato, and B. K. A. Ray, "Note on moving average forecasts of long memory processes with an application to quality control," *International Journal of Forecasting*, vol. 18, pp. 291–297, 2002.
[24] J. N. Pan and S. T. Chen, "Monitoring long-memory air quality data using ARFIMA model," *Environmetrics*, vol. 19, pp. 209–219, 2008.
[25] L. Rabyk and W. Schmid, "EWMA control charts for detecting changes in the mean of a long-memory process," *Metrika*, vol. 79, pp. 267–301, 2016.
[26] A. Muhammad, "A mixed EWMA-CUSUM control chart for weibull-distributed quality characteristics," *Quality and Reliability Engineering International*, vol. 32, no. 8, pp. 2987–2994, 2016.
[27] A. Muhammad, A. Muhammad, and J. Chi-Hyuck, "A HEWMA-CUSUM control chart for the weibull distribution," *Communications in Statistics - Theory and Methods*, vol. 47, no. 24, pp. 5973–5985, 2018.
[28] D. Brook and D.A. Evans, "An approach to the probability distribution of the CUSUM run

length," *Biometrika*, vol. 59, no. 3, pp. 539–549, 1972.

[29] D. M. Hawkins, "Evaluation of average run lengths of cumulative sum charts for an arbitrary data distribution," *Communications in Statistics Simulation and Computation*, vol. 21, pp. 1001–1020, 1992.

[30] C. W. Champ and S. E. Rigdon, "A comparison of the markov chain and the integral equation approaches for evaluating the run length distribution of quality control charts," *Communications in Statistics Simulation and Computation*, vol. 20, pp. 191–204. 1991.

[31] J. E. Wieringa, "Statistical process control for serially correlated data," Ph.D. dissertation, Faculty of Economics and Business, University of Groningen, Netherlands, 1999.

[32] C. A. Acosta-Mejía, J. J. Pignatiello, and B. V. Rao, "A comparison of control charting procedures for monitoring process dispersion," *IIE Transactions*, vol. 31, pp. 569–579, 1999.

[33] S. Knoth, "Computation of the ARL for CUSUM-S2 schemes," *Computational Statistics & Data Analysis*, vol. 51, pp. 499–512, 2006.

[34] W. Peerajit, Y. Areepong, and S. Sukparungsee, "Numerical integral equation method for ARL of CUSUM chart for long-memory process with non-seasonal and seasonal ARFIMA models," *Thailand Statistician*, vol. 6, no. 1, pp. 26–37, 2018.

[35] W. Peerajit and Y. Areepong, "The performance of CUSUM control chart for monitoring process mean for autoregressive moving average with exogenous variable model," *Applied Science and Engineering Progress*, vol. 15, no. 1, 2022, Art. no. 3490, doi: 10.14416/j.asep.2020.11.007.

[36] W. Peerajit, "Cumulative sum control chart applied to monitor shifts in the mean of a long-memory ARFIMAX(p,d^*,q,r) process with exponential white noise," *Thailand Statistician*, vol. 20, no. 1, pp. 144–161, 2022.

[37] P. Phanthuna and Y. Areepong, "Analytical solutions of ARL for SAR(p)L model on a modified EWMA chart," *Mathematics and Statistics*, vol. 9, no. 5, pp. 685–696, 2021.

[38] R. Sunthornwat, Y. Areepong, and S. Sukparungsee, "Average run length with a practical investigation of estimating parameters of the EWMA control chart on the long memory AFRIMA process," *Thailand Statistician*, vol. 16, no. 2, pp. 190–202, 2018.

[39] A. Muhammad, S. Ambreen, A. Mohammed, M.-M. Jean-Claude, and C. S. Sandile, "A new CUSUM control chart under uncertainty with applications in petroleum and meteorology," *Plos One*, vol. 16, no. 2, 2021, Art. no. e0246185.